New Developments in 3D Analytical Electron Tomography

Zineb Saghi

email: zineb.saghi@cea.fr

With the contribution of: Guillaume Biagi, Martin Jacob, Audrey Jannaud, Gabriele Navarro, Mei-Lin Grouzelle, Frédéric Lorut, Jean-Luc Starck and Philippe Ciuciu.

3D CHARACTERIZATION TECHNIQUES AT THE NANOSCALE

Atom probe tomography	Electron tomography	Slice-and-view tomography

Field ion microscope combined with a mass spectrometer

Transmission electron microscope (TEM)

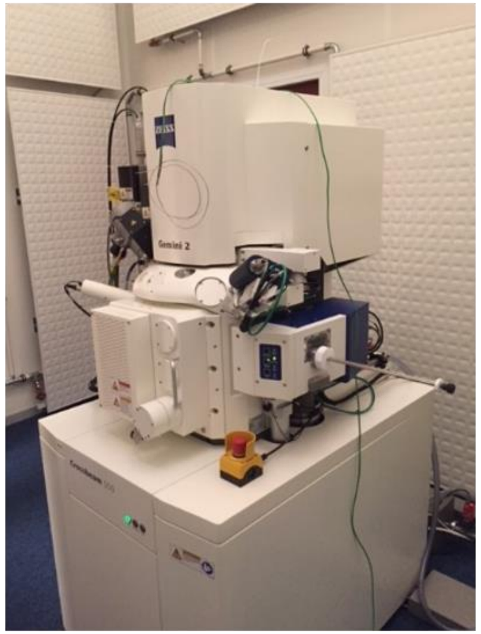

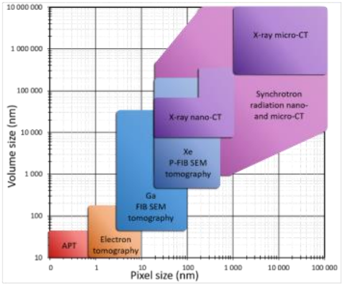

Focussed ion beam combined with a scanning electron microscope (FIB-SEM)

BASICS OF ELECTRON TOMOGRAPHY

- In electron tomography, 3D volumes are reconstructed from a set of 2D projections acquired inside a transmission electron microscope.
- *Very promising* technique for the 3D analysis of semiconductor materials and devices, catalytic systems, polymers, biological structures, etc.
- Well-established for 3D *morphological* analysis.

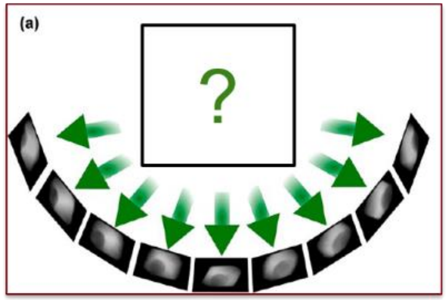

1. Acquisition

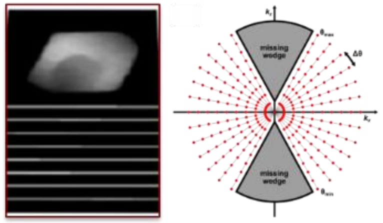

2. Alignment

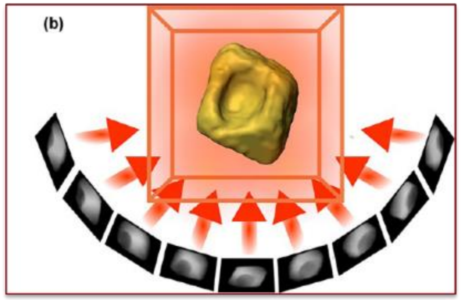

3. Reconstruction

HAADF-STEM tilt series
-90°:1°:+90°

3D HAADF-STEM reconstruction

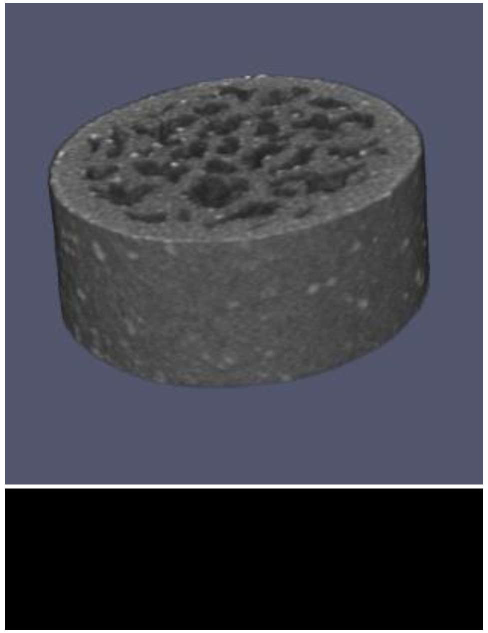

HAADF-STEM tomography of an Er-doped porous silicon structure (G. Mula et al. Scientific Reports 2017, 7:5957)

ANALYTICAL ELECTRON TOMOGRAPHY USING MODERN TEMs

Advances in instrumentation:

- High-brightness sources (Cold and Schottky-type field emission guns)
- EDX detectors with large solid angles (>0.7sr) and high detection efficiency (Silicon drift detectors).
- EELS spectrometers with high-speed (>1000 spectra/s) and high-performance electronics (direct detection technology).

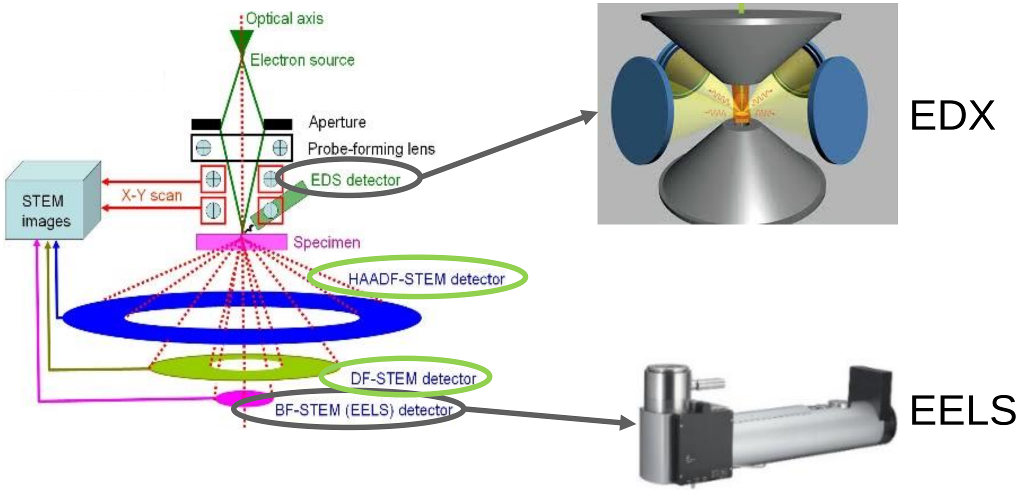

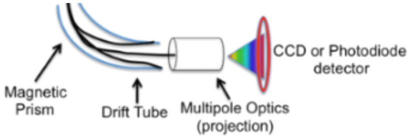

EDX: Energy-dispersive X-ray spectroscopy
EELS: Electron energy loss spectroscopy

Analytical electron tomography using EELS and/or EDS modes:

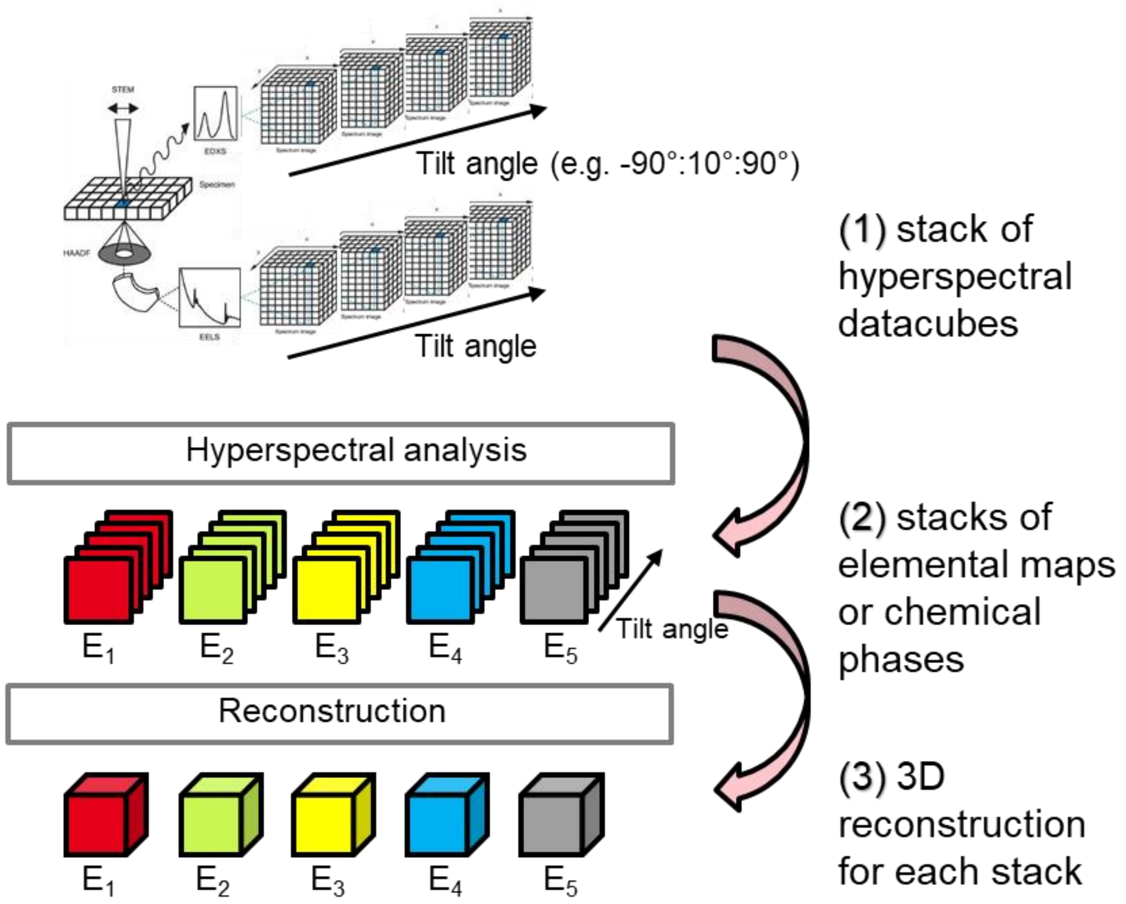

CHALLENGES RELATED TO ANALYTICAL ELECTRON TOMOGRAPHY

Long acquisition times
High electron doses

(Manual acquisition)

Limited number of projections
Low SNR spectra

Acquisition

Typical acquisition parameters:

HAADF-STEM tomography:
Probe current: 100pA
Tilt angles: -90°:1°:+90°
Frame size: 2048x2048 pixels
Frame time: 20sec.

STEM-EDX tomography:
Probe current: 200pA-1nA
Tilt angles: -90°:10°:+90°
Frame size: 300x300 pixels.
Acquisition time: 15min.

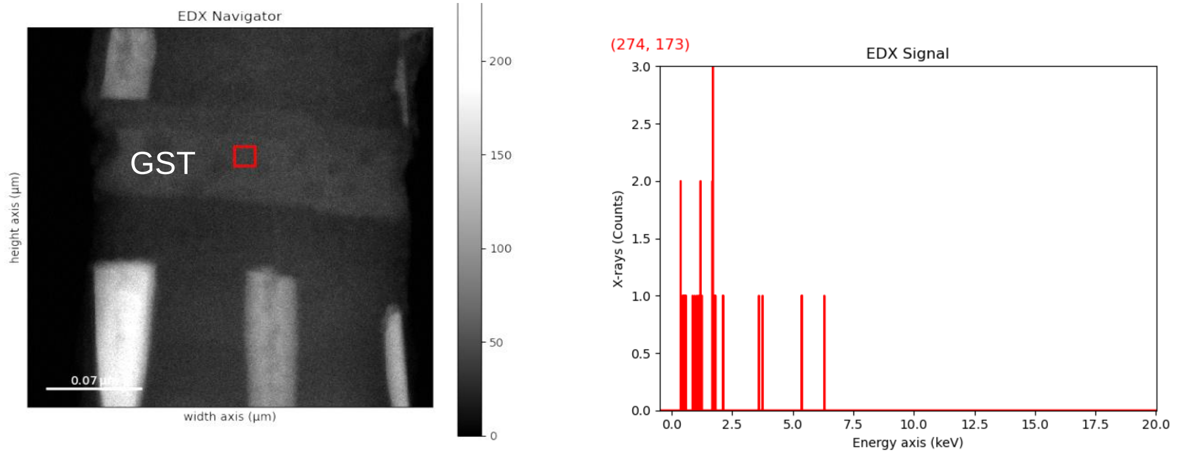

STEM-EDX hyperspectral image.

Data processing

Commercial software **not optimized** for:
Tomographic spectral analysis
3D reconstruction with undersampled data

OUTLINE

- Fast and automated hyperspectral analysis of tomographic datasets (EELS/EDX)
- Overview of advanced reconstruction algorithms
- Applications of analytical ET:
  - As-doped silicon structure.
  - Ge-Sb-Te (GST)-based phase-change materials.
- Future prospects
  - Hybrid/correlative studies
  - Deep learning for 3D reconstruction under low-dose, limited-angle and sparse-view conditions

FAST AND AUTOMATED HYPERSPECTRAL ANALYSIS OF TOMOGRAPHIC DATASETS (EELS/EDX)

HyperSpy
multi-dimensional data analysis

- Tools to import and batch process the full tomographic stack of EELS and/or EDX datacubes

- Denoising by principal component analysis (PCA)

- Elemental mapping :
  - Conventional approach (background subtration and peak integration)
  - Curve fitting approach (useful for peak separation, no need for a precise spectrum calibration)

- Chemical phase mapping (spectral unmixing approach)**:**
  - Independent component analysis (ICA)
  - Non-negative matrix factorization (NMF)
  - Vertex component analysis (VCA)

Number of components estimation :
Prior knowledge on the observed sample.
PCA scree-plot.

PCA scree-plot

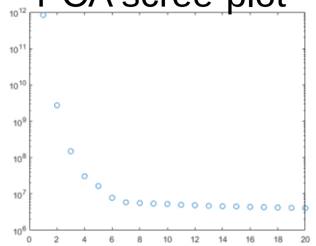

APPLICATIONS OF MULTIVARIATE STATISTICAL ANALYSIS METHODS

3D visualization of iron oxidation state by STEM-EELS tomography

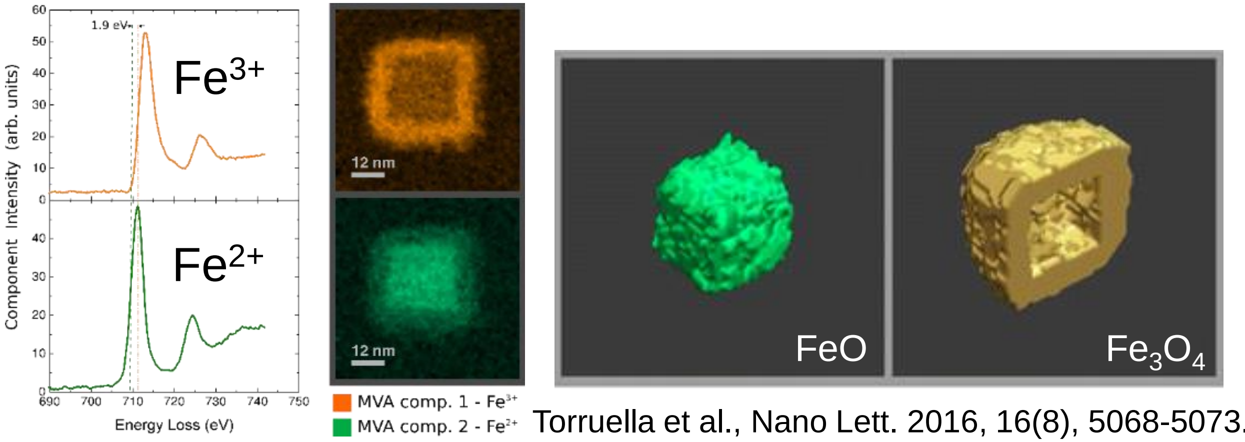

Torruella et al., Nano Lett. 2016, 16(8), 5068-5073.

EDX-STEM tomography of nickel-based superalloy

D. Rossouw et al., Acta Materialia 2016, 107, 229-238.

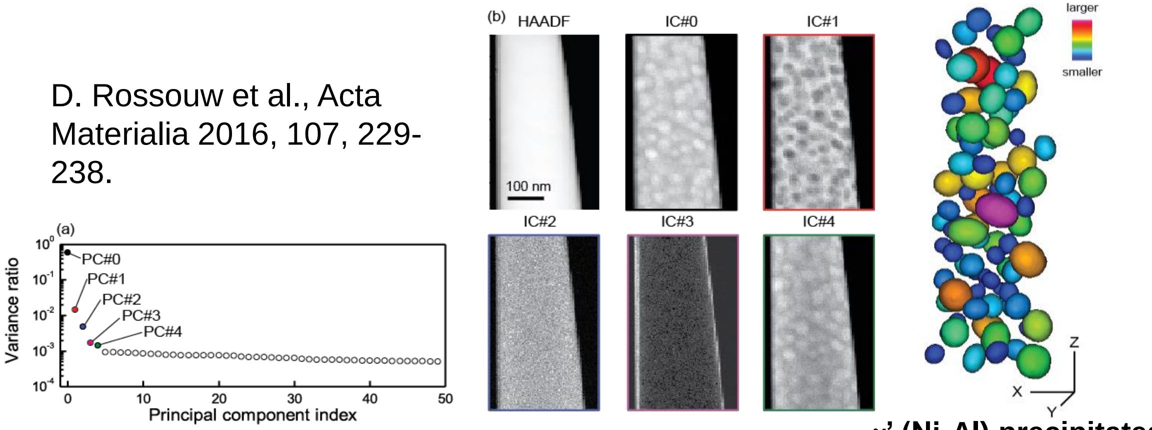

γ' (Ni_3Al) precipitates

Ag nanocube localised surface plasmon resonances by STEM-EELS tomography

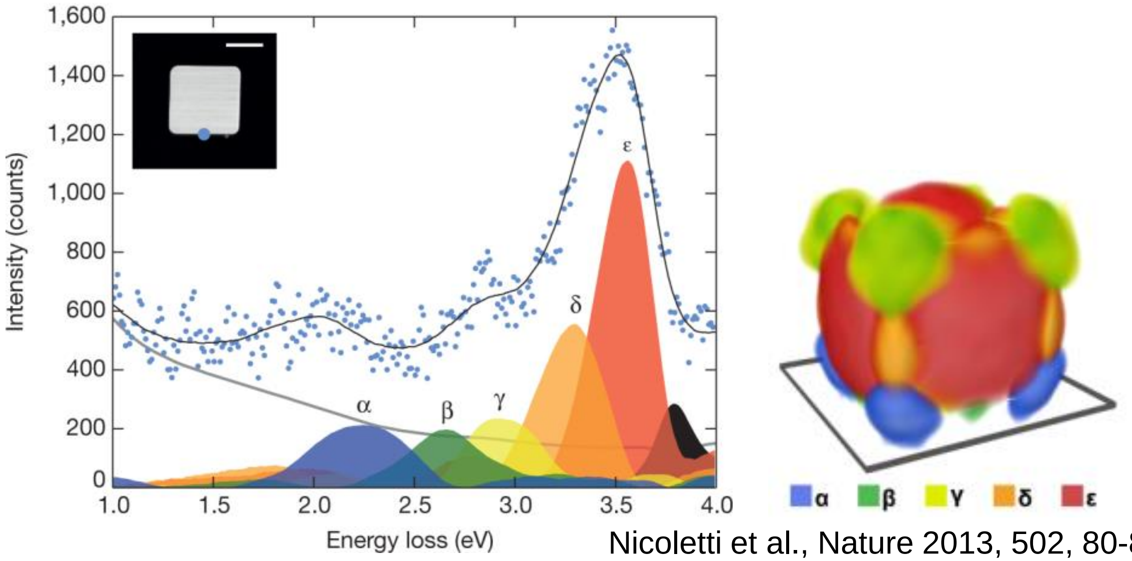

Nicoletti et al., Nature 2013, 502, 80-84.

Scanning precession electron tomography of Ni-based superalloy

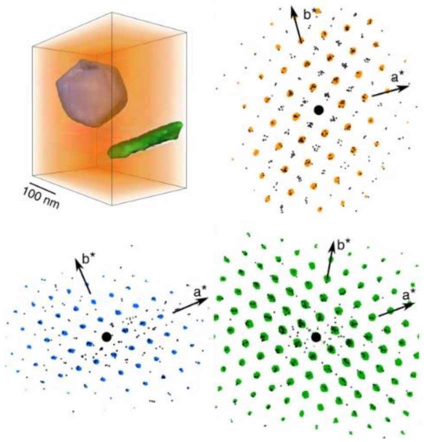

4,000,000 diffraction patterns in total….

- Component diffraction patterns - phase specific
- Reconstruct component virtual dark field images
- Real + reciprocal space crystallographic tomography!

Eggeman et al., Nat. Comms. 2015, 6, 7267.

EDX-STEM TOMOGRAPHY OF A HIGH ELECTRON MOBILITY TRANSISTOR USING NON-NEGATIVE MATRIX FACTORIZATION (NMF)

Study of Ti- and Al-Rich Contact Metallization for AlGaN/GaN high electron mobility transistors

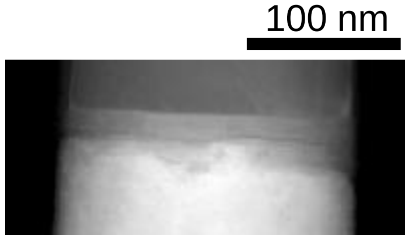

HAADF-STEM

37 EDX-STEM projections
103x200 pixels
5min/map

STEM-EDX tomography

NMF + alignment and reconstruction of the different chemical phase volumes

Data processing

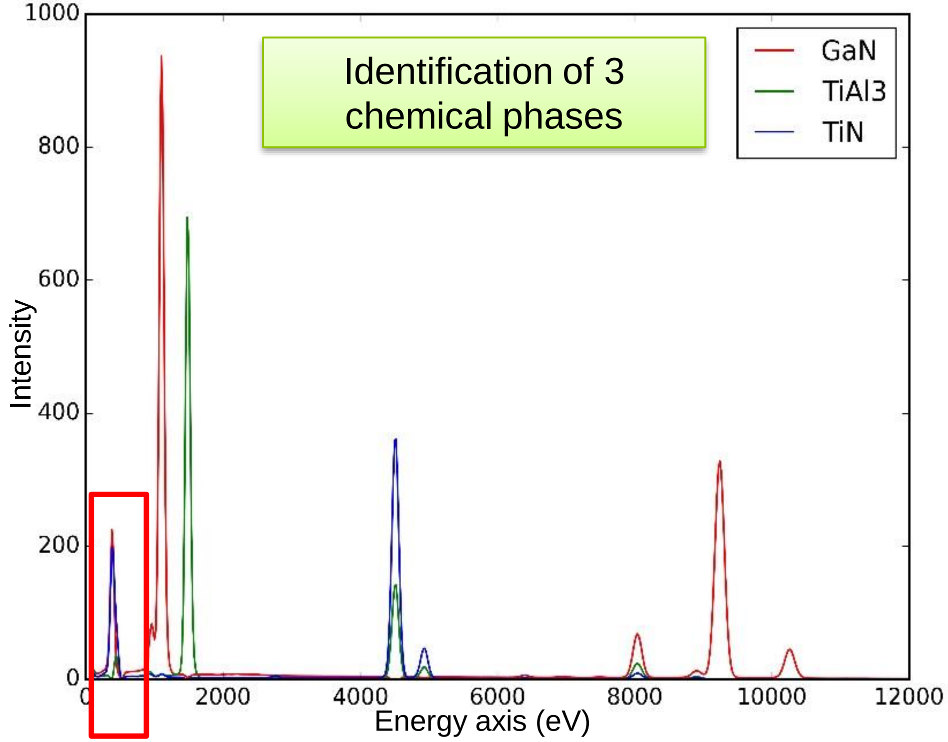

Spectral unmixing of the tomographic STEM-EDX dataset

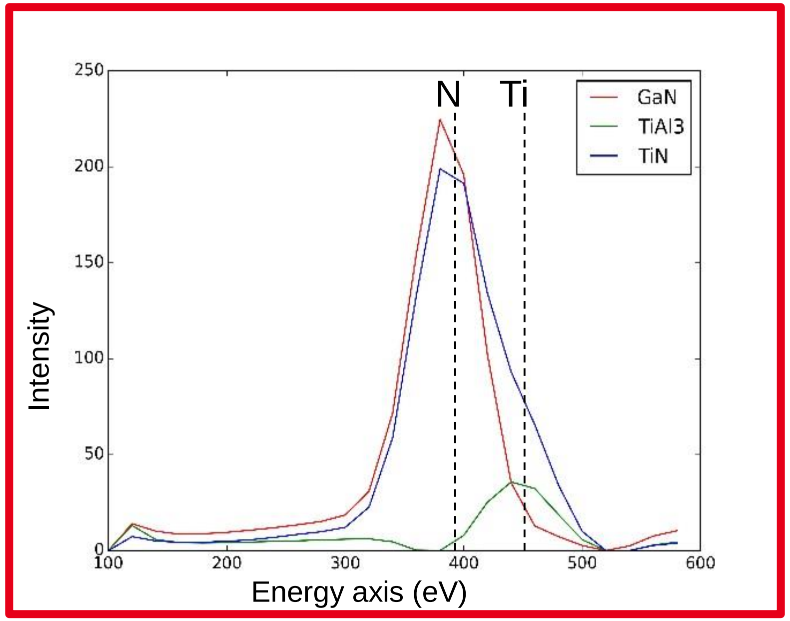

Aligned tilt series

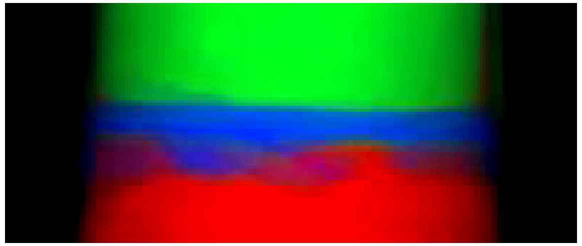

GaN $TiAl_3$ TiN

Slices through the 3D reconstruction

OUTLINE

- Fast and automated hyperspectral analysis of tomographic datasets (EELS/EDX)
- **Overview of advanced reconstruction algorithms**
- Applications:
  - As-doped silicon structure.
  - Ge-Sb-Te (GST)-based phase-change materials.
- Future prospects
  - Hybrid/correlative studies
  - Deep learning for 3D reconstruction under low-dose, limited-angle and sparse-view conditions

CONVENTIONAL ALGORITHM: SIMULTANEOUS ITERATIVE RECONSTRUCTION TECHNIQUE (SIRT)

SIRT solves the following least squares problem:

$$\underset{x}{\operatorname{argmin}} \left\{ \frac{1}{2} \| Px - y \|_2^2 \right\}$$

Projection matrix (P)

The object to reconstruct (x)

Experimental data (y)

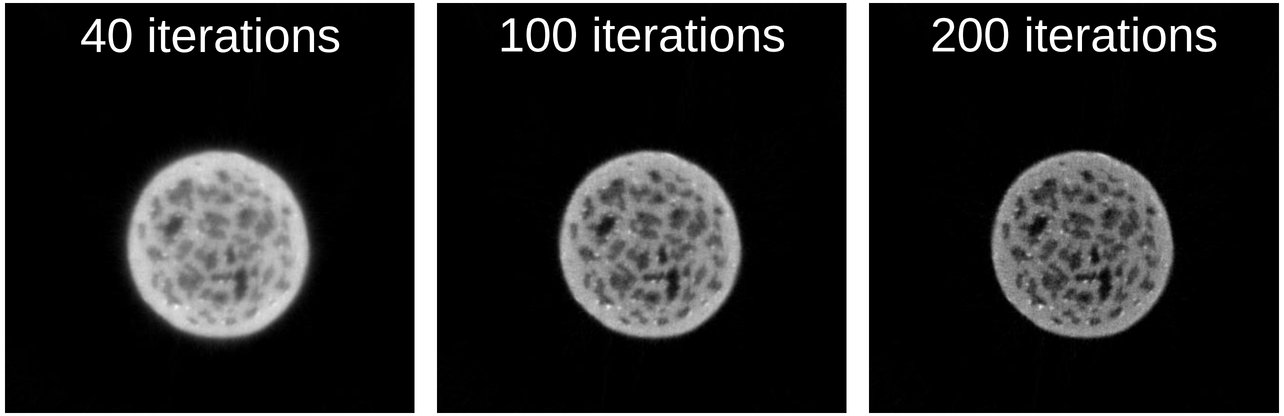

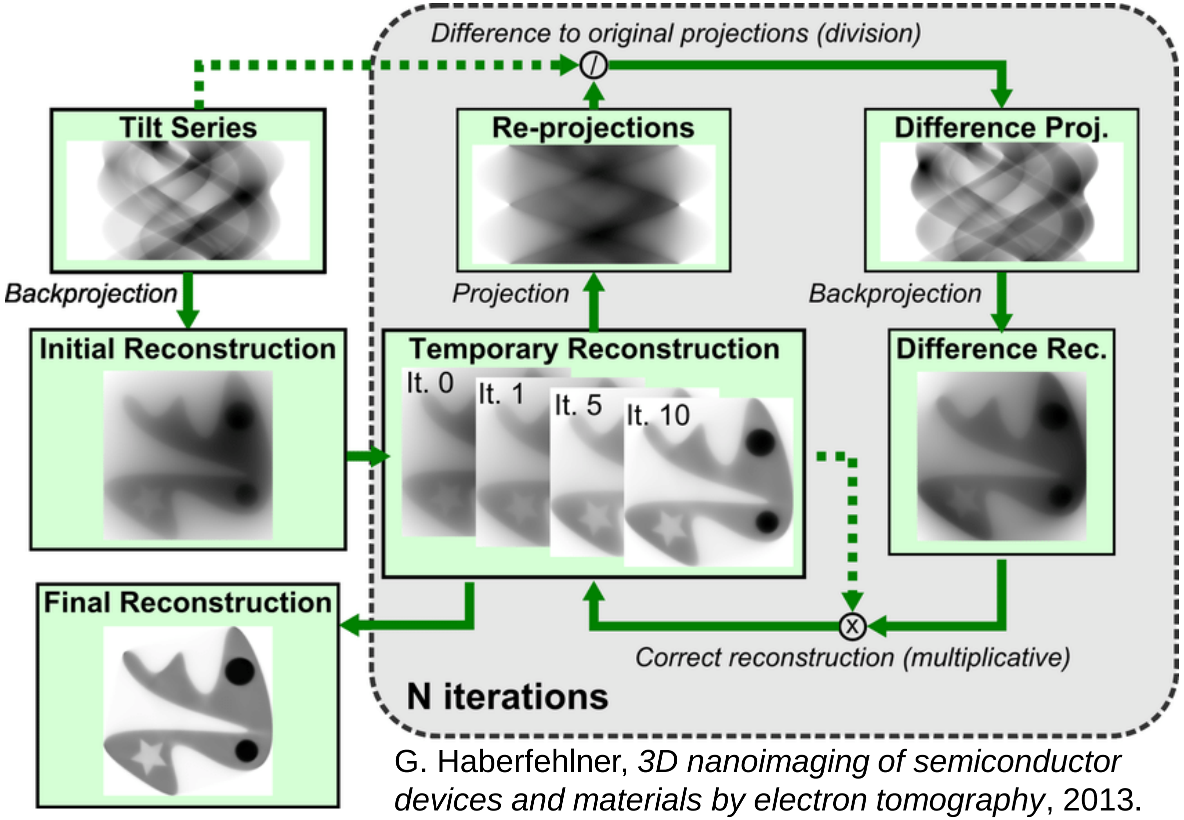

G. Haberfehlner, *3D nanoimaging of semiconductor devices and materials by electron tomography*, 2013.

C.OS. Sorzano et al., Biomed Res Int. 2017, 6482567.

SIMULTANEOUS ITERATIVE RECONSTRUCTION TECHNIQUE (SIRT)

Very limited number of projections

⇩

Poor-quality reconstructions

⇩

Unreliable segmentation

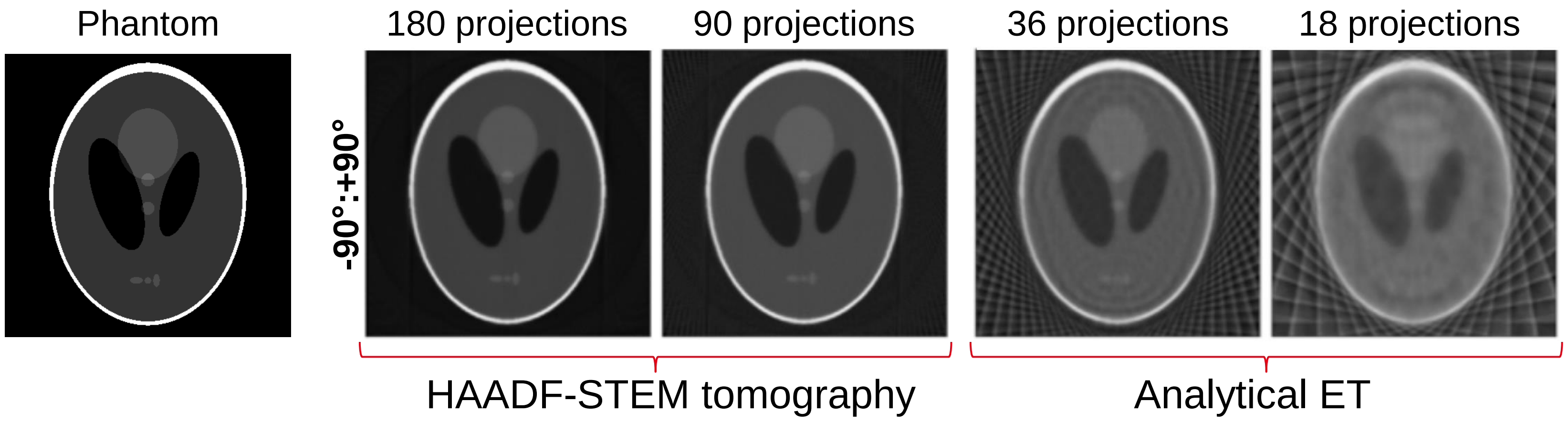

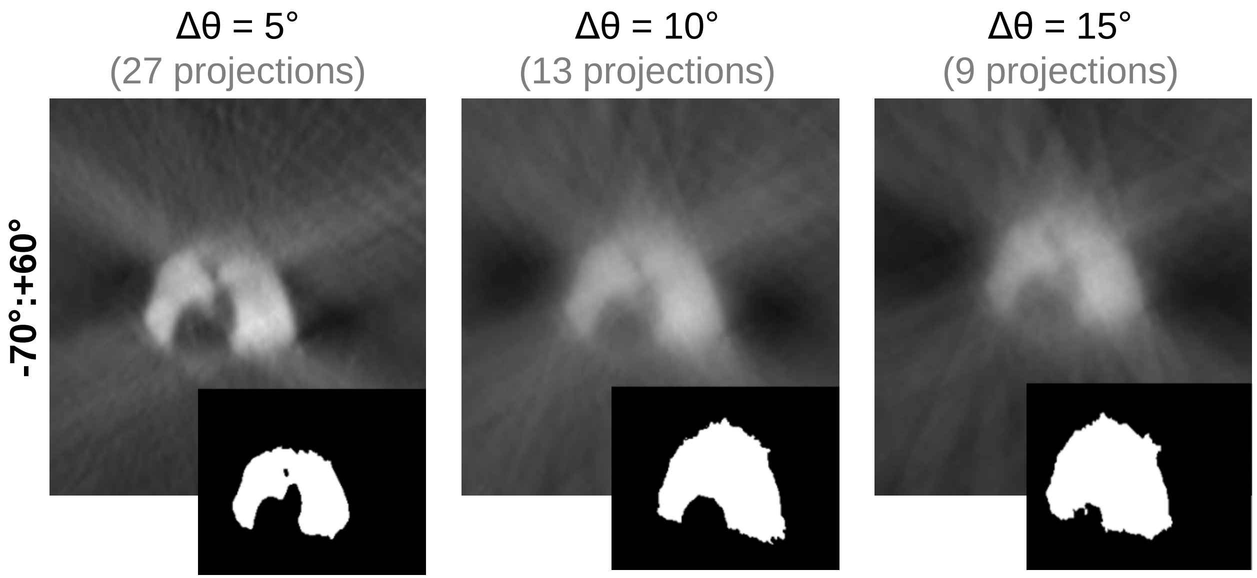

Z. Saghi et al., Nano Letters 2011, 11(11), 4666.
R. Leary et al., Ultramicroscopy 2013,131, 70.

Add prior knowledge

Discrete ART (DART)

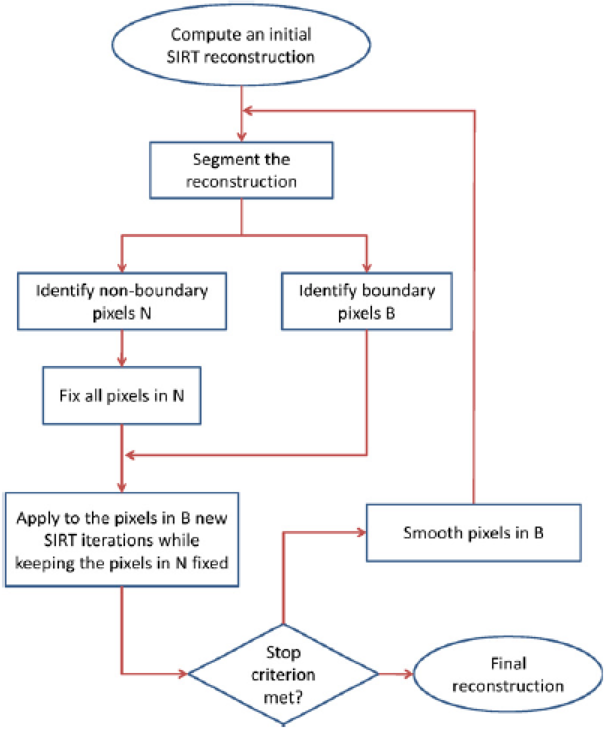

Fig. 2. Flow chart of the DART algorithm.

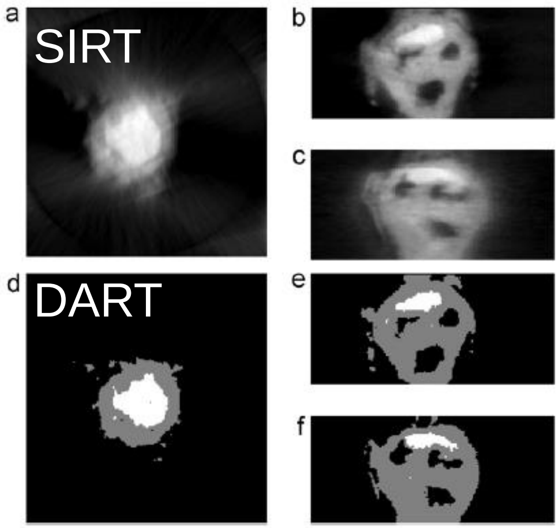

Prior knowledge: number of grey levels, and their intensities.

S. Bals et al. Nano Lett. 2007, 12, 3669
K.J. Batenburg et al. Ultramicrosc. 2009, 109, 730

Compressed sensing (CS)

$$\underset{x}{\operatorname{argmin}} \left\{ \frac{1}{2} \|Px - y\|_2^2 + \boldsymbol{\lambda \mathcal{R}(x)} \right\}$$

$\mathcal{R}(x) = \|Lx\|_0$ promotes sparsity of x in the transform domain L (few non-zero elements in Lx).

$$\underset{x}{\operatorname{argmin}} \left\{ \frac{1}{2} \|Px - y\|_2^2 + \lambda \|Lx\|_0 \right\}$$

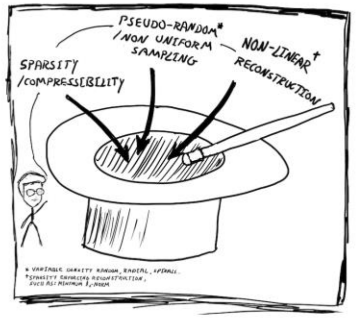

$$\underset{x}{\operatorname{argmin}} \left\{ \frac{1}{2} \|Px - y\|_2^2 + \lambda \|Lx\|_1 \right\}$$

SPARSITY IN THE GRADIENT DOMAIN

Total variation minimization (TV):
TV promotes sparsity in the gradient domain and is very well suited for objects with *piecewise constant regions and sharp edges*

$$\hat{f} = \underset{f}{argmin}\, \boldsymbol{\lambda} \|\boldsymbol{f}\|_{\boldsymbol{TV}} + \|\mathbb{R}f - p\|_2^2$$

with: $\|f\|_{TV} = \int |\nabla f(x)| dx$

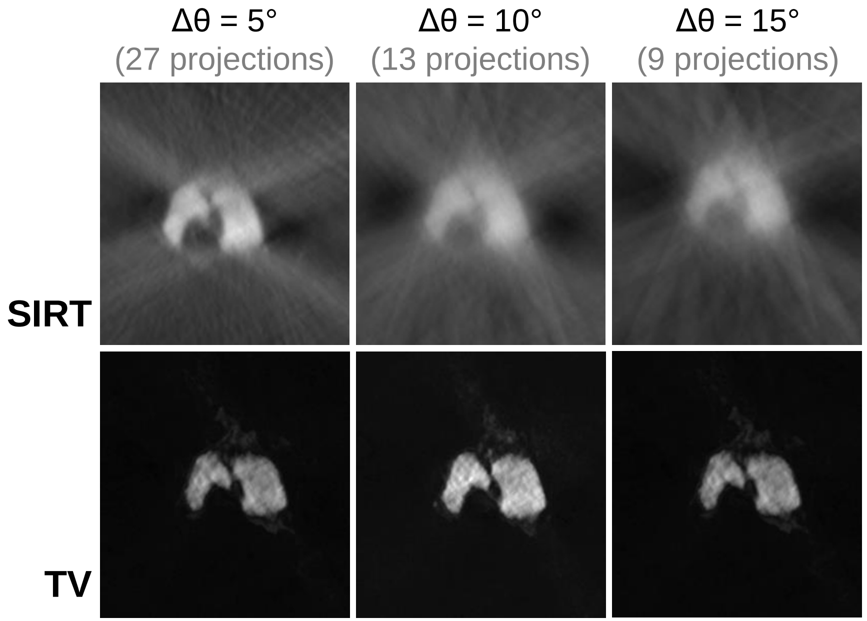

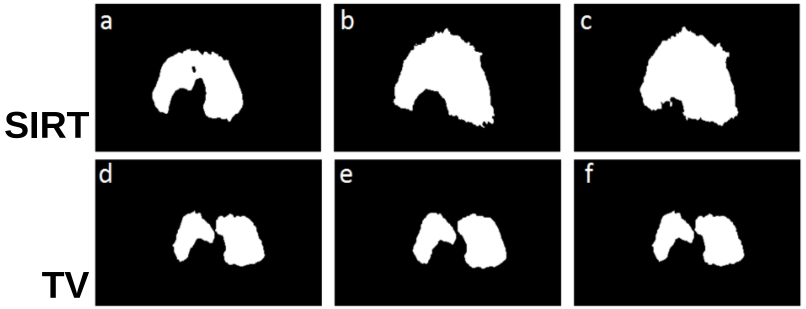

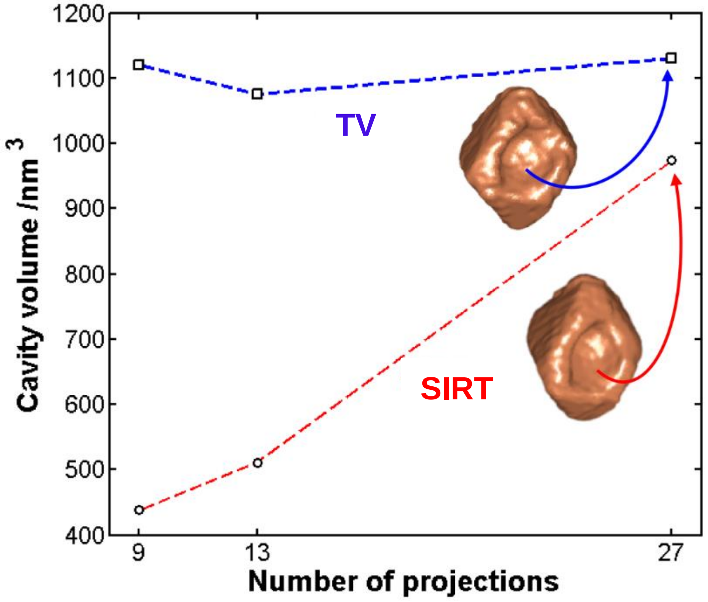

Z. Saghi et al., Nano Letters 2011, 11(11), 4666.
R. Leary et al., Ultramicroscopy 2013,131, 70.

SPARSITY IN THE GRADIENT DOMAIN

Limitations of TV:

- **Staircase artefacts** when the object is not truely piecewise constant.
- **Complex structures** require more projections than reported for simple objects (Y. Jiang et al. Ultramicrosc. 2017, 186)
- The quality of the reconstructions degrade rapidly in the presence of **Poisson noise**.

Higher order TV (Incorporation of higher order derivatives):

- **HOTV** (ref: R. Archibald et al. J. Sci. Comput. 2015, 67)
- **TGV** (total generalized variation, see e.g.: M. Benning et al. J. Sci. Comput. 2013, 54:269)
- Promote **piecewise smooth regions** while preserving sharp edges.

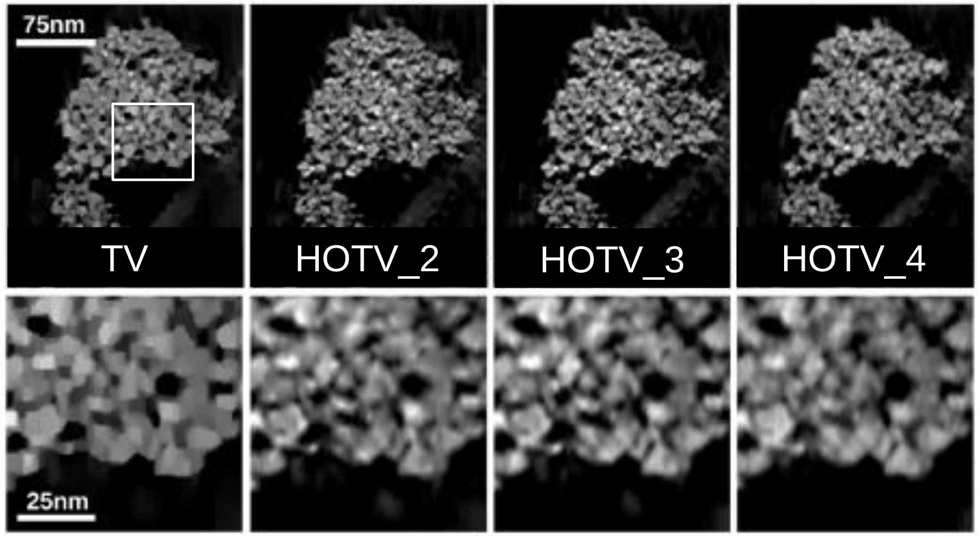

T. Sanders et al., Ultramicrosc. 2017, 174, 97.

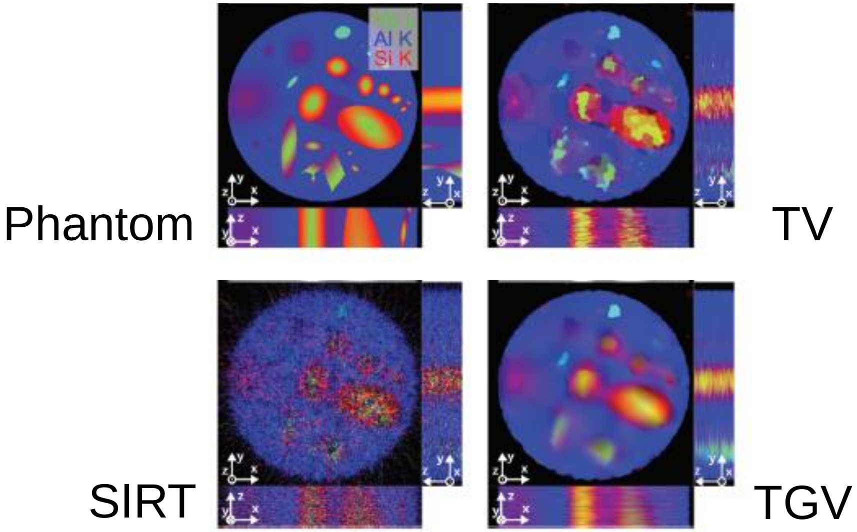

R. Huber et al., Nanoscale 2019, 11, 5617.

SPARSITY IN THE WAVELET DOMAIN

Sparsity in the wavelet domain:

- Multiscale approach used in microscopy mainly for denoising purposes.
- Widely used in MRI and recently applied to CT and ET.
- Applied to a wider range of objects, compared to gradient sparsity.
- Knowledge about the sample => choice of the appropriate wavelet function.

First application in spectroscopic ET (using coiflets wavelets)

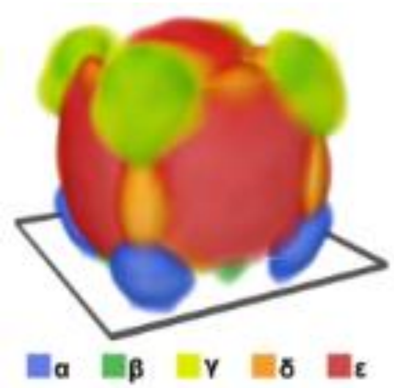

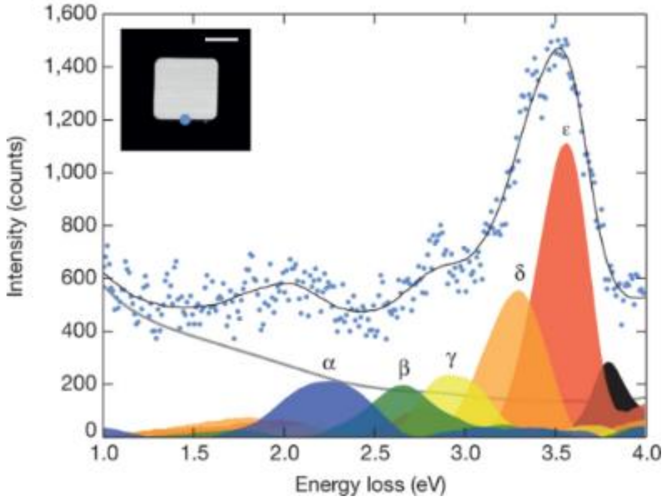

Three-dimensional imaging of localized surface plasmon resonances of metal nanoparticles.
Nicoletti *et al.* Nature 2013, 502, 80.

Haar wavelets

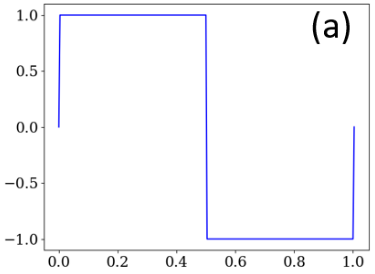

(multi-scale gradient)

Undecimated biorthogonal wavelets

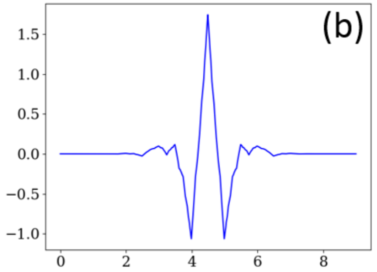

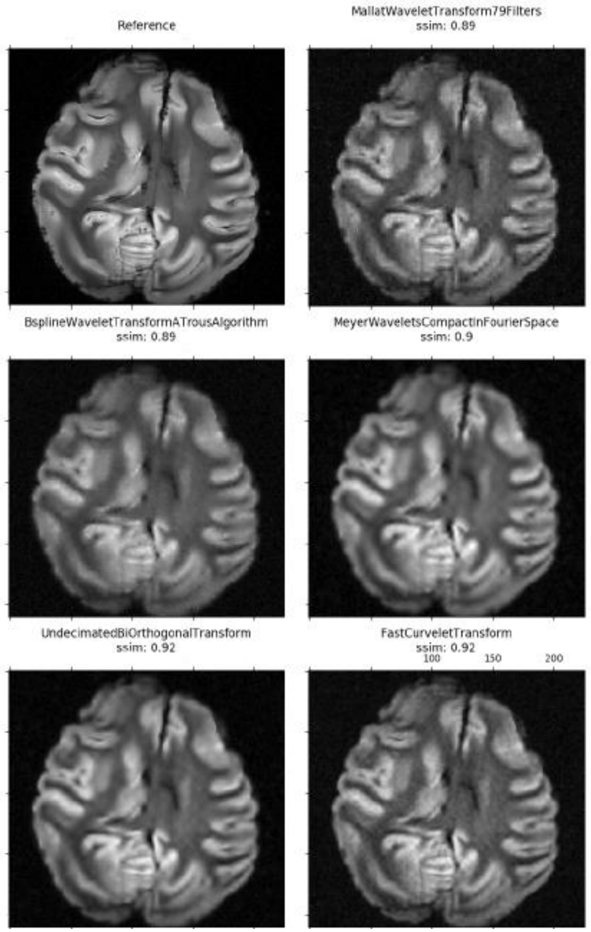

H. Cherkaoui et al. EUSIPCO 2018, 36.

PYSAP-ETOMO: AN OPEN-SOURCE TOOLBOX FOR COMPRESSED SENSING ELECTRON TOMOGRAPHY

MRI

Frequency domain

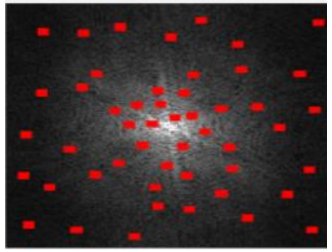

ET

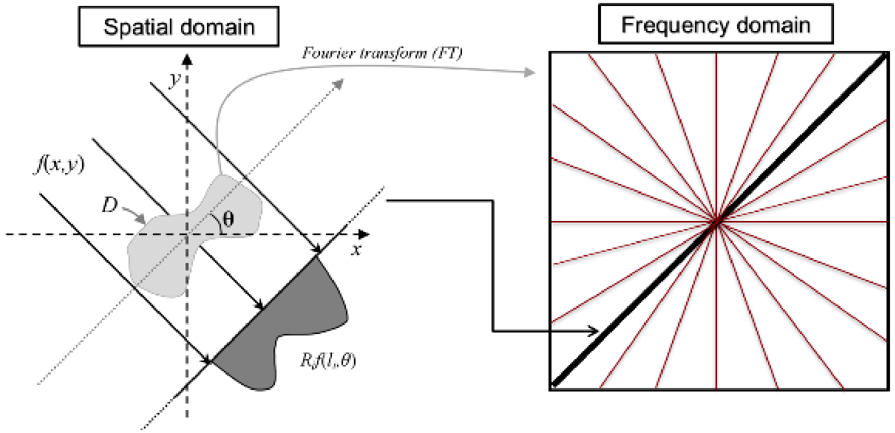

$$\underset{x}{argmin}\left\{\frac{1}{2}\|\boldsymbol{P}x-y\|_2^2+\lambda\|\boldsymbol{R}x\|_1\right\}$$

Optimization algorithms	Projection operators	Sparsity transforms
Proximal gradient methods: *FISTA* *POGM* **Primal-dual methods:** Condat-Vu **Options:** Positivity constraint Soft thresholding and reweighting	**Fourier-based:** Non-uniform FFT **Radon-based:** *Radon transform and the back-projection operator*	**Gradient-based:** TV HOTV *TGV* **Wavelet-based:** Pywavelets (e.g.: Haar, Bior4.4) *Sparse2D* *(e.g.: Ridgelets, Curvelets)*

Packages imported: Astra, PyNUFFT, Pywavelets and Modopt.

https://github.com/CEA-COSMIC/pysap-etomo

Collaboration with CEA-Neurospin (MRI)

M. Jacob et al., Ultramicroscopy 2021, 255, 113289.

OTHER OPEN-SOURCE PACKAGES FOR 3D RECONSTRUCTION

Name	General features	Reconstruction algorithms
Astra toolbox	Initially developed for X-ray tomography GPU-based implementations. Incorporated in Inspect3D (FEI)	Standard reconstruction algorithms + TV plugin
Tomopy	Initially developed for X-ray tomography CPU-based implementations. Recently integrated with Astra toolbox.	Standard reconstruction algorithms
Tomotools	Developed for electron tomography Tools for alignment + reconstruction.	Standard reconstruction algorithms (Astra + Tomopy)
Tomviz	Open source plateform for alignment, reconstruction and visualization.	Standard reconstruction algorithms + TV
Matlab package (T. Sanders et al., Ultramicroscopy 2017, 174: 97)	Alignment, inpainting and denoising.	TV, HOTV, and multiscale HOTV.
Graptor (R. Huber et al., Nanoscale 2019, 11:5617)	Developed for EELS/EDS tomography GPU-based implementations.	TGV algorithm and multi-modal reconstruction approach
PySAP-etomo (M. Jacob et al., Ultramicroscopy 2021, 255: 113289)	*Adaptation of PySAP + Modop libraries* *Includes Astra and Pywavelet.*	*Implementation of gradient-based (TV, TGV, HOTV) and wavelet-based methods.*

COMPARISON OF VARIOUS SPARSITY TRANSFORMS

Dataset: Er-doped porous Si structure
HAADF-STEM mode
Tilt angles: -90°:1°:+89°

TV/Haar: staircasing artifacts due to the piecewise constancy assumption.

HOTV_3 : no staircasing artifacts. Noise-like oscillations appear with large tilt increments.

Bior4.4: best results. Induces smoothness with large tilt increments

Effect of angular under-sampling

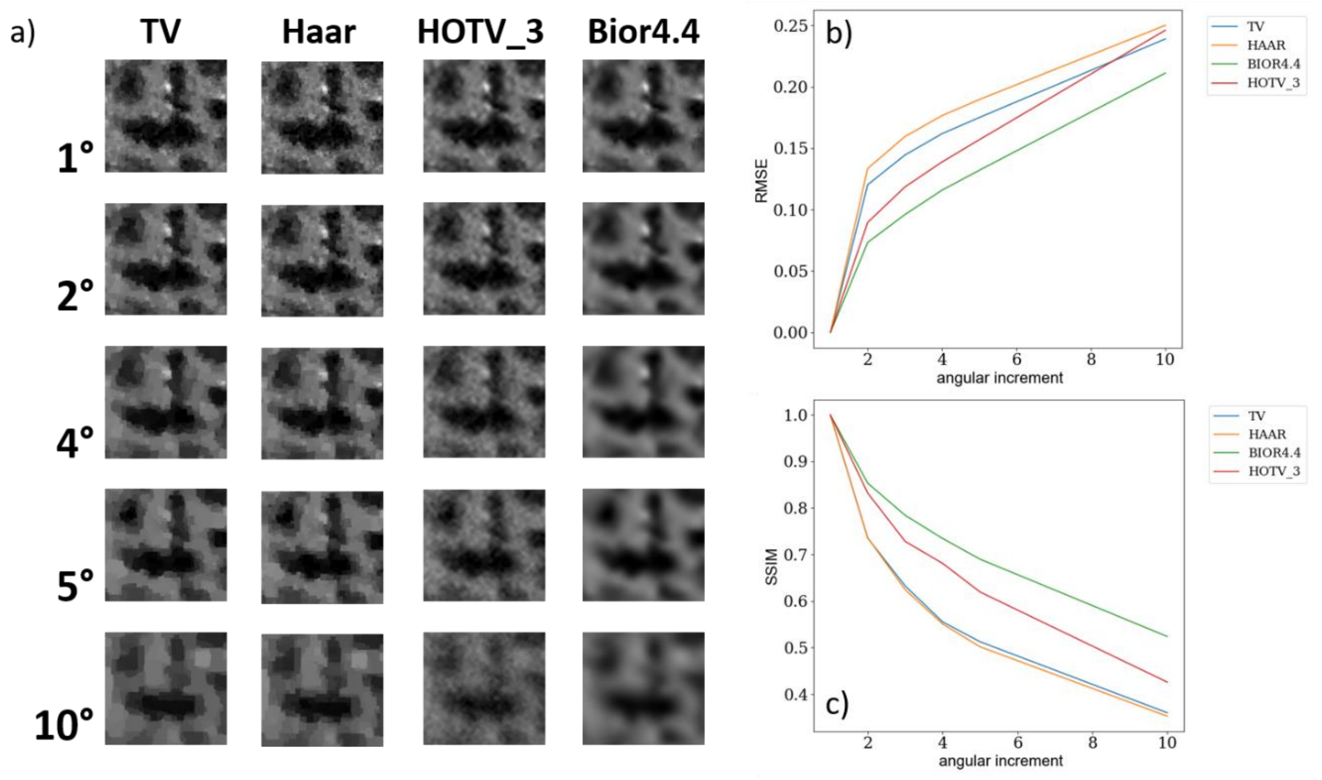

TV, Haar, HOTV_3 and Bior4.4 reconstructions with 1°, 2°, 4°, 5° and 10° increments. (b) RMSE and (c) SSIM scores showing the evolution of the image quality as function of the angular increment (in degrees).

HAADF-STEM AND EDX-STEM TOMOGRAPHY OF AS-DOPED SI FIN-SHAPED STRUCTURE

Aim of the study:
- Conformality of As implantation.
- Dopant depth profiling in 3D.
- Roughness of the sidewalls of the structure.

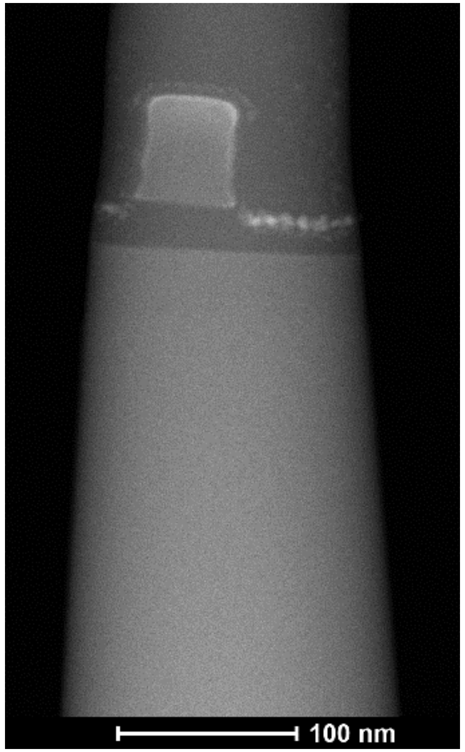

HAADF-STEM acquisition:
- Tilt series: -90°:5°:+90°
- Frame size: 2048x2048 pixels
- Pixel size : 0.26nm
- 15sec frame time

EDS-STEM acquisition
- Tilt series: -90°:10°:+90°
- Datacube size: 193x163x2048
- Pixel size : 1nm
- 10min frame time

Data processing
- NMF
- CS reconstruction using TV

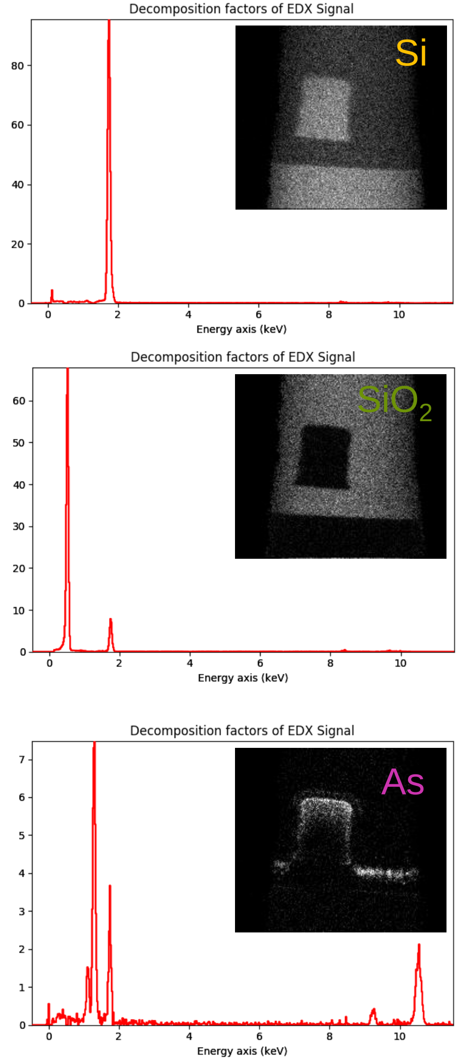

Chemical phase analysis by NMF

HAADF-STEM AND EDX-STEM TOMOGRAPHY OF AS-DOPED SI FIN-SHAPED STRUCTURE

HAADF-STEM tomography
3D information about sidewall roughness

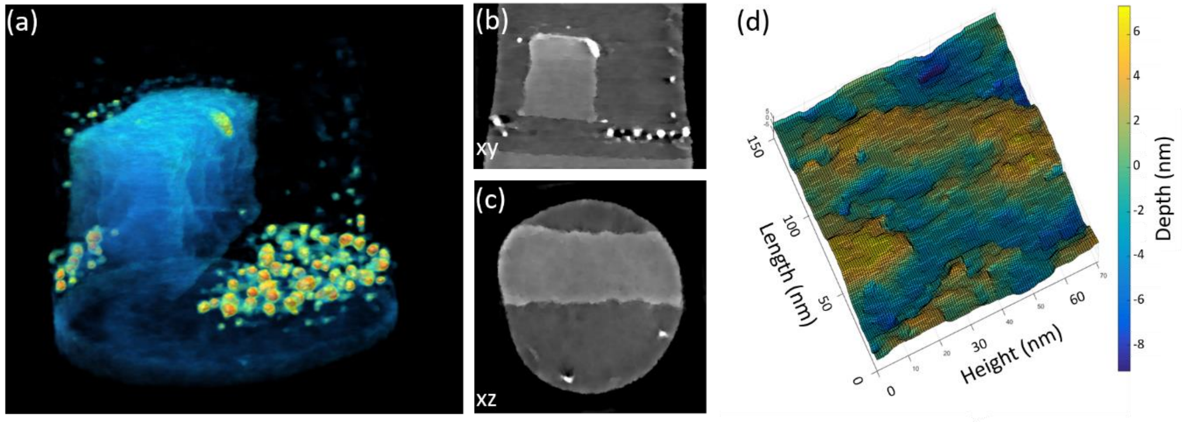

STEM-EDX tomography
3D information about As implantation

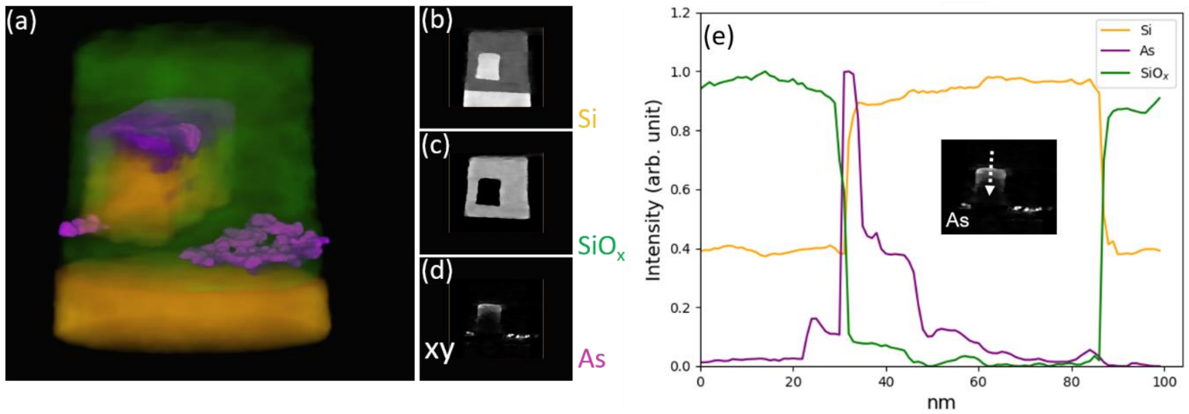

	STEM-EDX tomography	STEM-HAADF tomography
RMS roughness	-	~3 nm
Average precipitate volume	~20 nm^3	~15 nm^3
As implantation depth	~20 nm	-

M. Jacob et al., Semicond. Sci. Technol. 2021, 36, 035006.

STEM-EELS TOMOGRAPHY OF A GE-RICH GE-SB-TE (GST) THIN FILM FOR PHASE-CHANGE MEMORY (PCM) APPLICATIONS

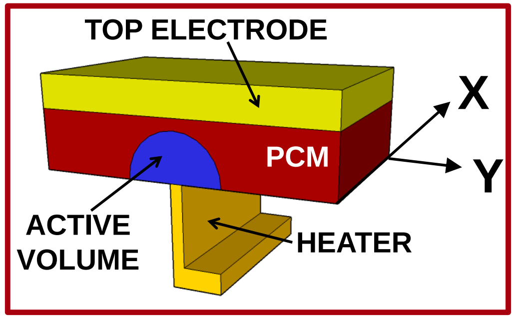

Example of an industrial PCM device

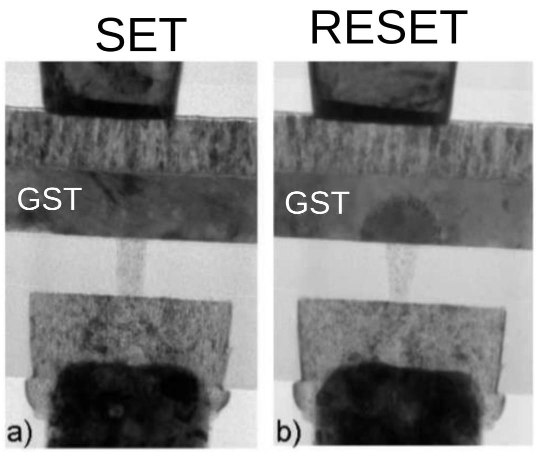

From: Phase change materials: science and applications, S. Raoux and M. Wuttig, Springer Verlag, New York, 2009.

Current challenge: PCM memory devices stability is challenged at high temperature (automotive applications).

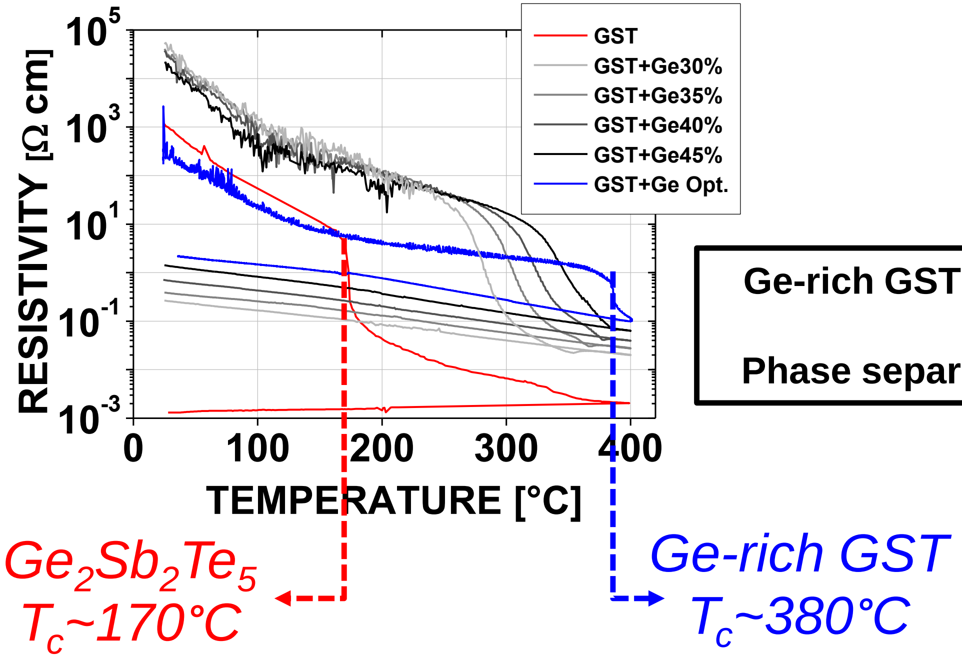

Ge-rich GST crystallisation

⇩

Phase separation GST & Ge

Increase of Ge at. %

⇩

Increase of crystallization temperature (T_c)

STEM-EELS TOMOGRAPHY OF A GE-RICH GE-SB-TE (GST) THIN FILM FOR PHASE-CHANGE MEMORY (PCM) APPLICATIONS

HAADF-STEM (-90°:5°:+90°): 1024x1024 pixels, pixel size: 0.53nm, frame time: 16.7sec.

STEM-EELS (-90°:10°:+90°): 100x75 pixels, pixel size: 2.04nm, exposure time: 0.1sec (450eV, 1eV/ch), SI acquisition time: 18min.

Data processing: VCA + CS reconstruction using TV, Haar, HOTV_3 and undecimated biorthogonal wavelets (Bior4.4)

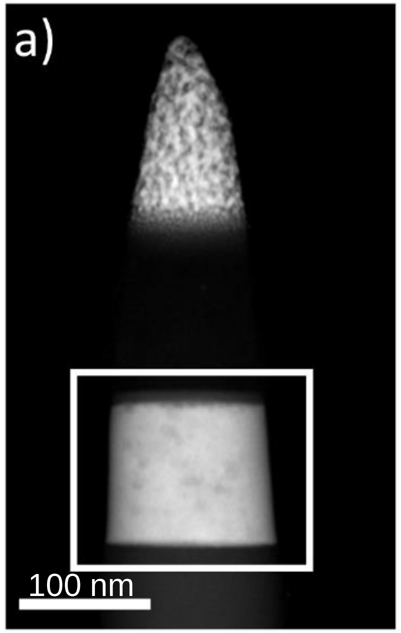

VCA decomposition

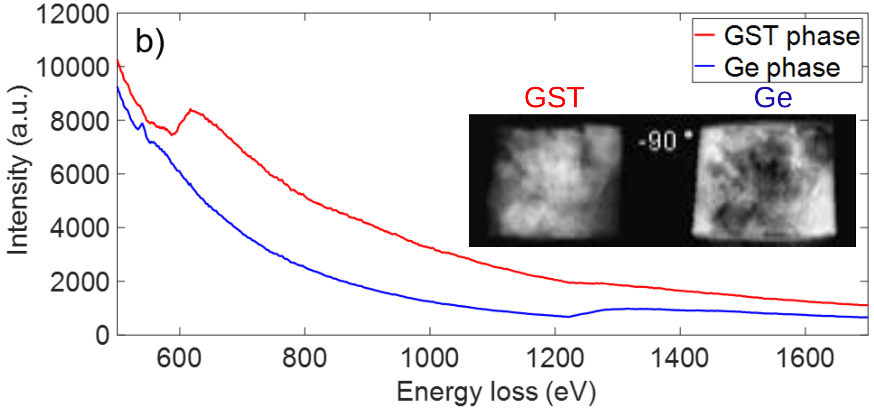

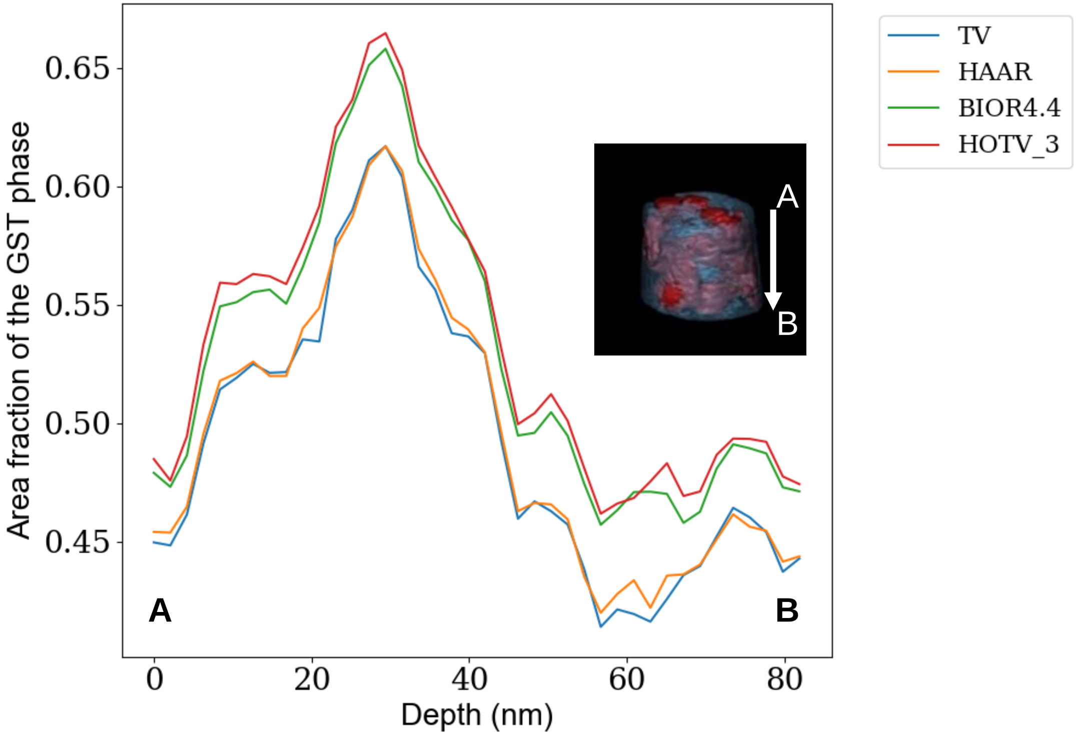

Volume fraction of the GST phase:

Bior4.4: 0.527 Haar: 0.494
HOTV_3: 0.533 TV: 0.491

M. Jacob et al., Ultramicroscopy 2021, 255: 113289

A HYBRID APPROACH FOR IMPROVING THE QUALITY OF EDX-STEM RECONSTRUCTIONS

HEBT: HAADF-EDS bimodal tomographic reconstruction. Assumption: HAADF-STEM projection images are the linear sum of the EDX maps for all present elements.

TGV coupled: joint multi-channel reconstruction of HAADF and EDX data. Assumption: similar interface positions for all reconstructions.

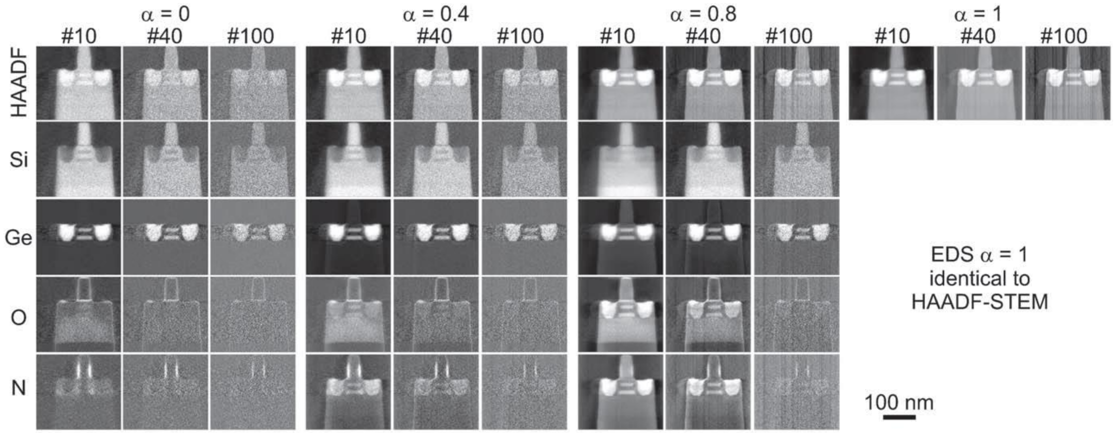

HEBT approach
H. Bender et al., Semicond. Sci. Technol. 2019, 34, 114002.

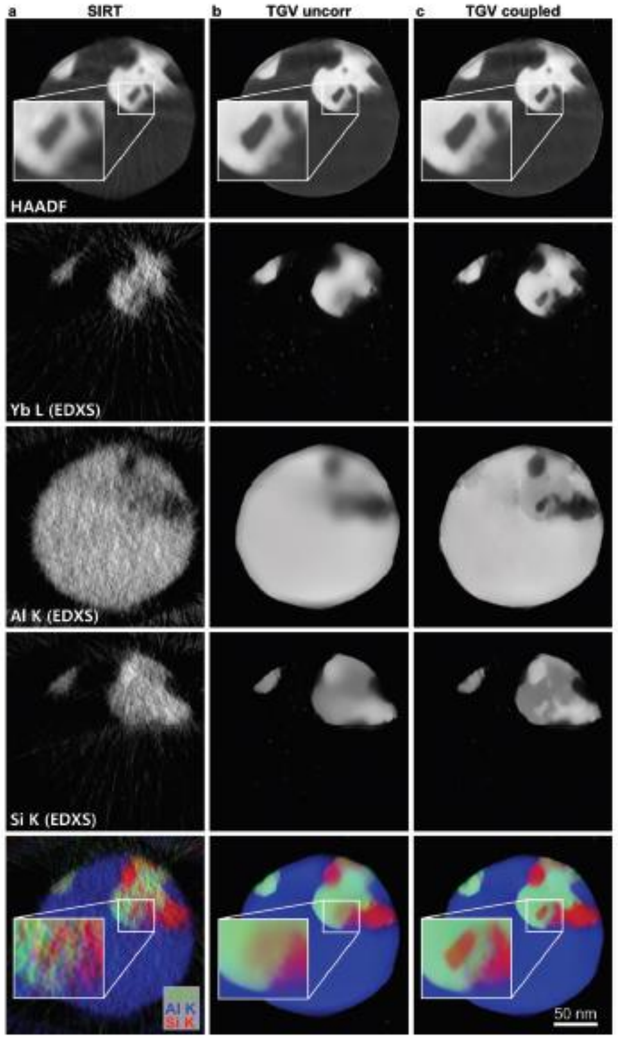

TGV coupled approach
R. Huber et al., Nanoscale 2019, 11, 5617.

A HYBRID APPROACH FOR ABSORPTION CORRECTION IN STEM-EDX TOMOGRAPHY

uncorrected corrected

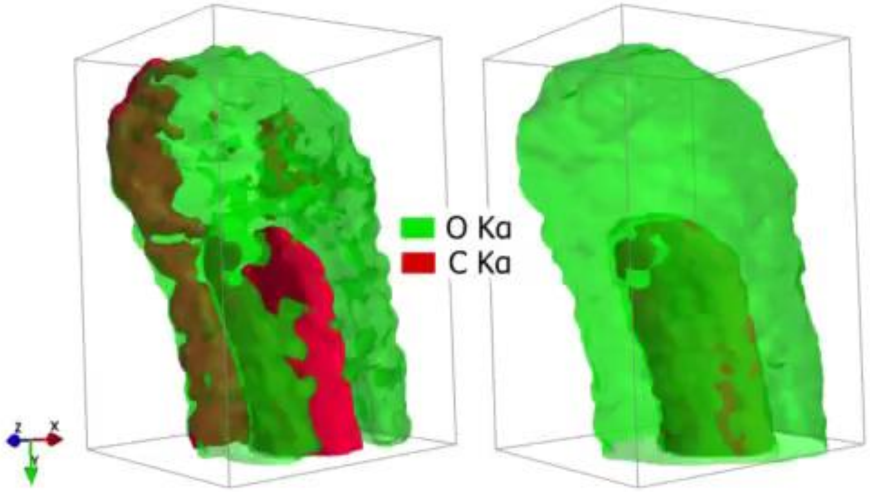

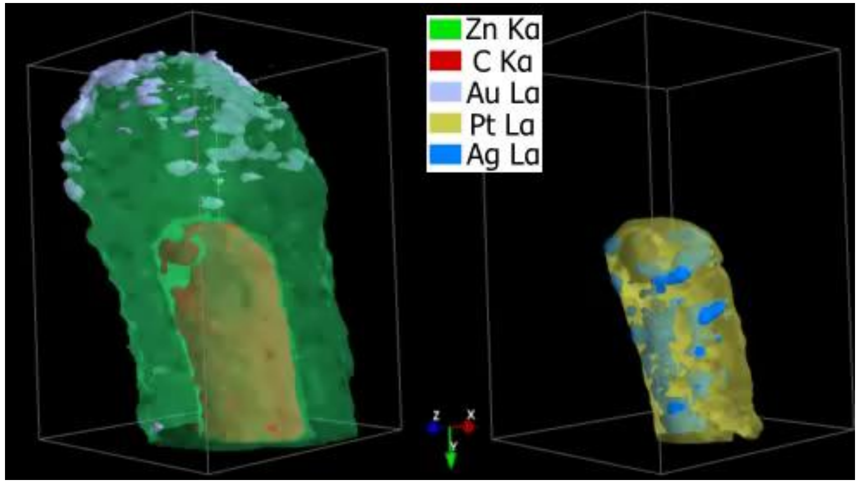

Burdet et al., Ultramicrosc. 2016, 160: 118

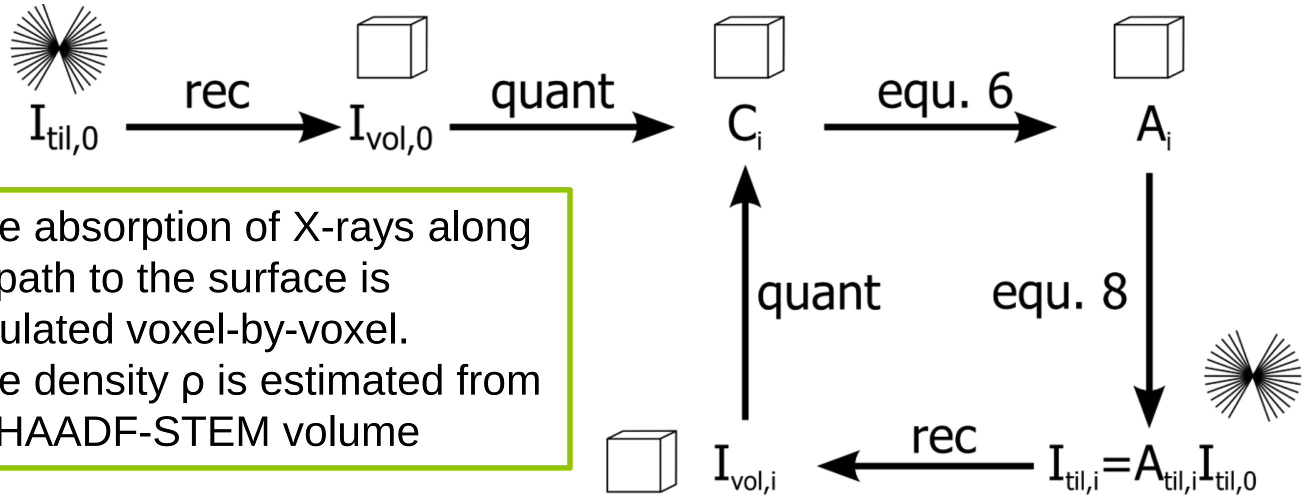

- The absorption of X-rays along the path to the surface is calculated voxel-by-voxel.
- The density ρ is estimated from the HAADF-STEM volume

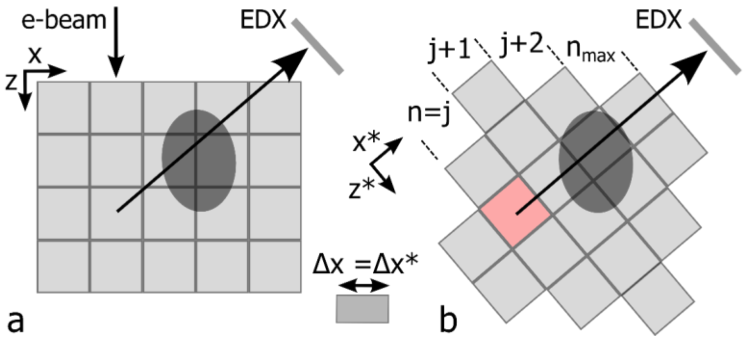

$$\frac{I}{I_j} = exp\left(-\sum_{n=j+1}^{n_{max}} \left[\frac{\mu}{\rho}\right]_n \rho_n \Delta x\right). \qquad (6)$$

$$\mathbf{A}_{til,i} = \frac{[\mathbf{I}_{vol,i}]_{til}}{[\mathbf{I}_{vol,0}]_{til}} = \frac{[\mathbf{I}_{vol,0}\mathbf{A}_i]_{til}}{[\mathbf{I}_{vol,0}]_{til}}, \qquad (8)$$

Detector geometry

Slater et al., Ultramicroscopy 162 (2016) 61–73
Xu et al., Ultramicroscopy 164 (2016) 51-61

FUTURE PROSPECTS: CORRELATIVE SPECTROSCOPIC ET/APT

EDX-STEM tomography

APT

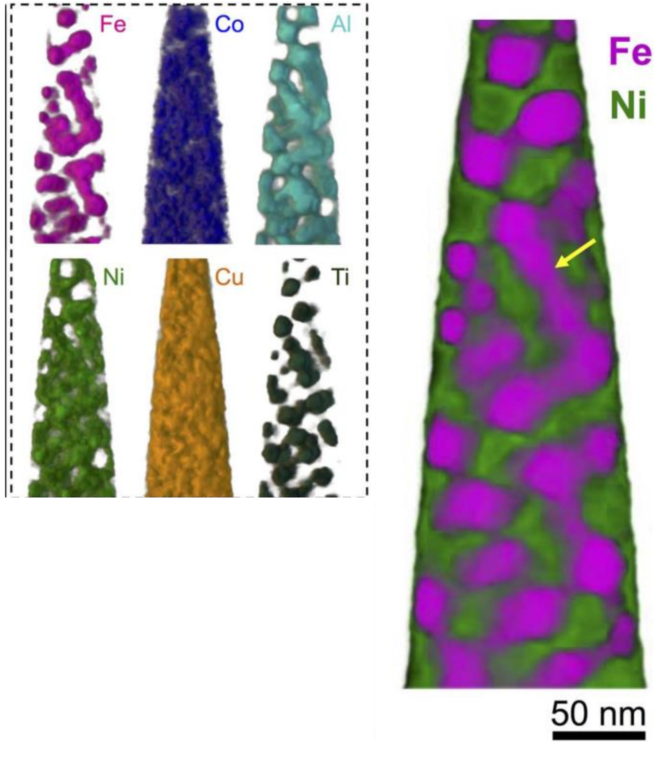

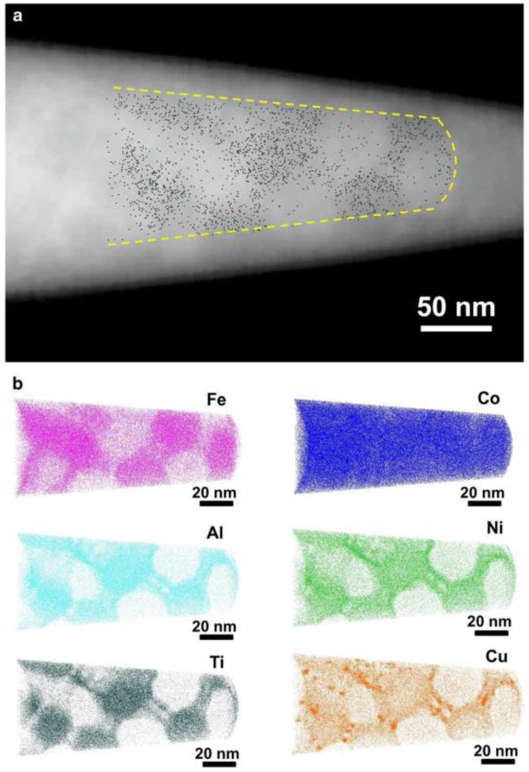

Phase Separation in an Alnico 8 Alloy.
Guo et al., Microsc. Microanal. 2016, 22, 1251.

EELS/EDX-STEM tomography:
Non-destructive, large fields of view, high spatial fidelity, limited spatial resolution (few nms), LLD ~1×10^{20} at.cm^{-3}, quantification methods not fully developped.

APT:
Destructive, small fields of view, limited spatial fidelity, high spatial resolution, LLD ~5×10^{18} at.cm^{-3}, quantitative method.

FUTURE PROSPECTS: DEEP LEARNING APPROACHES FOR LOW-DOSE AND LIMITED-ANGLE TOMOGRAPHY

Limited-angle tomography

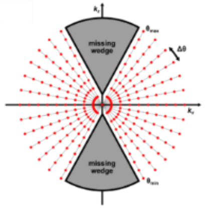

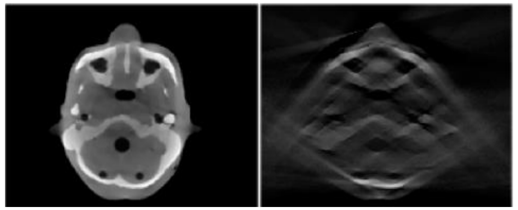

Reference | Standard algorithm (FBP)

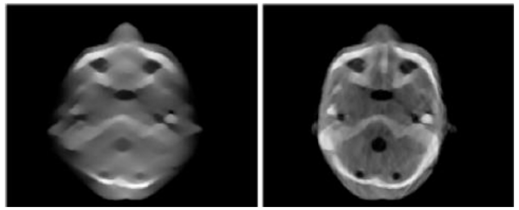

CS approach (TV) | DL approach (GAN)

Z. Li et al., Sensors 2019, 19, 3941.

Low-dose tomography

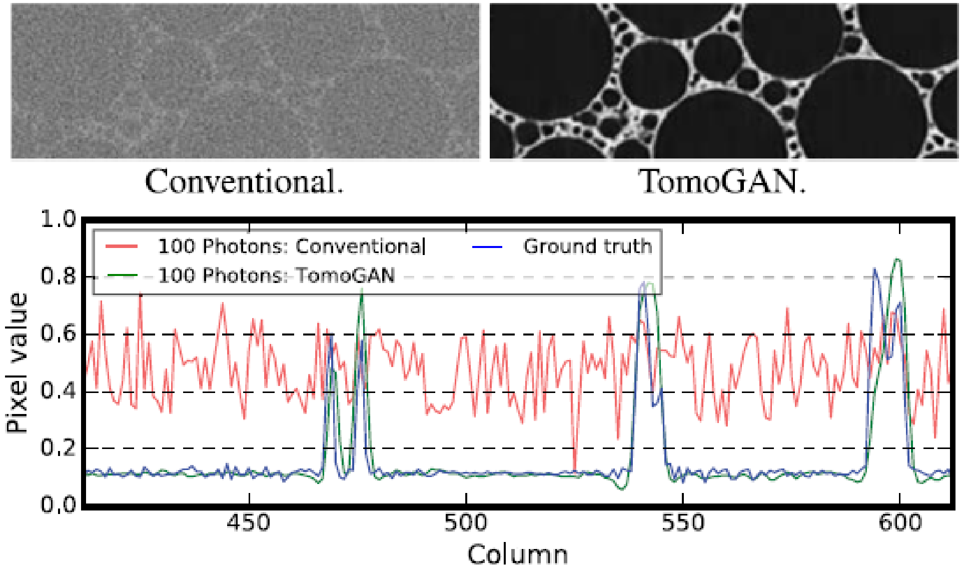

100 photons

Z. Liu et al., J. Opt. Soc. Am. A 2020, 37, 422.

DEEP LEARNING APPROACHES FOR ELECTRON TOMOGRAPHY

Porous structures

SIRT reconstruction | DL result

-90°:10°:90° no noise

-90°:3°:90° Noisy projections

-60°: 1°: 60° Noisy projections

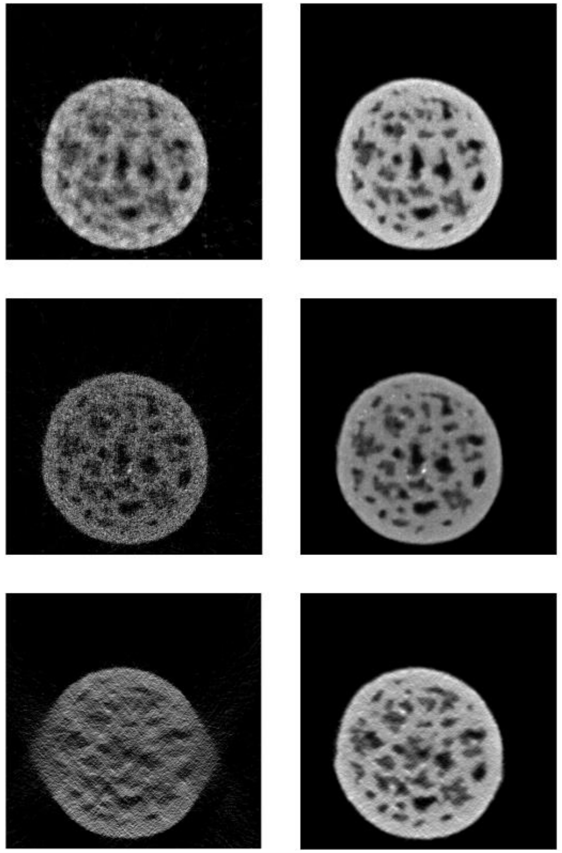

Reference image

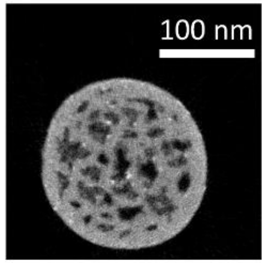

(SIRT reconstruction, -90°:1°:90°)

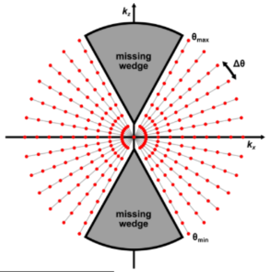

Tilt range	Number of projections	Poisson noise added	SIRT reconstruction PSNR / SSIM	DL output PSNR / SSIM
180°	18	no	22.5 / 0.782	25.8 / 0.807
180°	60	yes	19.8 / 0.675	26.1 / 0.806
120°	120	yes	19.6 / 0.633	25.8 / 0.823

Nanoparticles

-60°:1°:60°

SIRT reconstruction

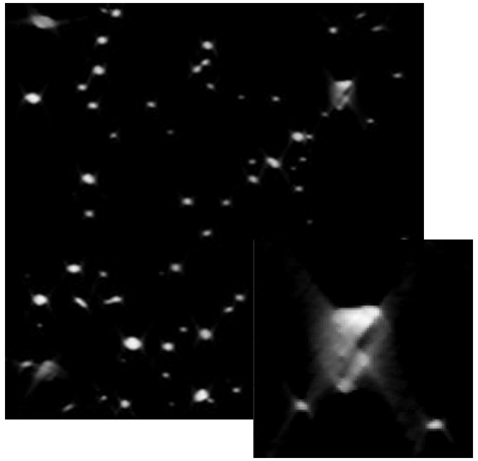

DL result

HAADF-STEM tomography of Pt catalysts (-59°:2°:63°)

SIRT reconstruction

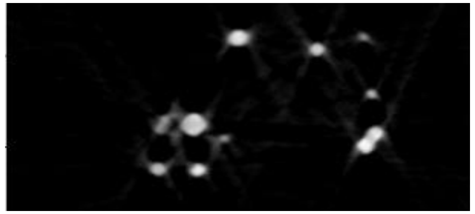

DL result

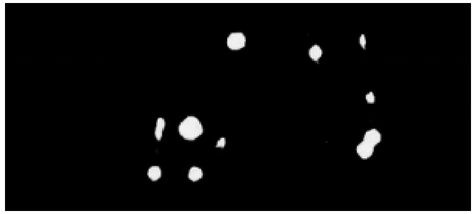

Correction of missing wedge artefacts

CONCLUSIONS

- Analytical ET is very promising for comprehensive semiconductor device analysis with 3D information about morphology *and* chemistry.

- Simultaneous EDX and precession electron diffraction was demonstrated in 2D and can be extend to 3D for more complete information (morphology + chemistry + *structure*).

- The technique will certainly evolve in the future, with continuous progress in:
  - Instrumentation (direct electron detectors, EDX systems with solid angles reaching 4 sr, EELS spectrometers with 8000 spectra/s, etc)
  - Data processing (machine learning tools for spectral analysis, reconstruction algorithms based on CS and DL)

- The correlation of analytical ET with APT is a promising route that can benefit both techniques.

- DL approaches are beginning to revolutionize ET (high-speed, low-dose, correction of missing wedge artifacts).

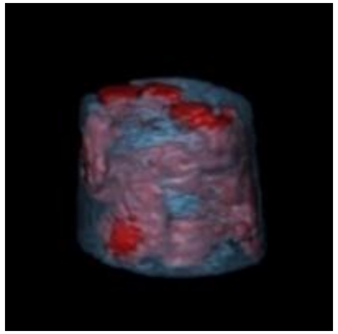

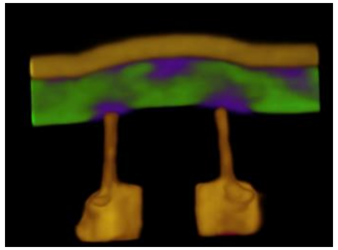

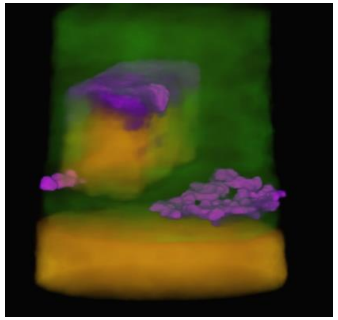

ACKNOWLEDGMENTS

CEA DRT/Leti/DPFT:
M. Jacob
M-L. Grouzelle
G. Biagi
A. Grenier
P. Quéméré

ST Crolles:
F. Lorut
A. Valery

CEA DRT/Leti/DCOS:
G. Navarro

CEA DRF/IRFU:
J-L. Starck
S. Farrens

CEA DRF/NEUROSPIN:
P. Ciuciu

Thank you for your attention!

Email: zineb.saghi@cea.fr